# Graphene/SOI-based self-powered Schottky barrier photodiode array (EP)

(iD) A. Yanilmaz, (iD) M. Fidan, (iD) O. Unverdi, et al.

**COLLECTIONS**

Paper published as part of the special topic on Photodetectors Based on Van der Waals Heterostructures and Hybrid 2D Materials

EP   This paper was selected as an Editor's Pick

View Online          Export Citation          CrossMark

---

**ARTICLES YOU MAY BE INTERESTED IN**

Topological sensor on a silicon chip
Applied Physics Letters **121**, 011101 (2022); https://doi.org/10.1063/5.0097129

Regulating the electronic structure of cobalt phosphide via dual-metal doping engineering to trigger efficient hydrogen evolution
Applied Physics Letters **121**, 013904 (2022); https://doi.org/10.1063/5.0098085
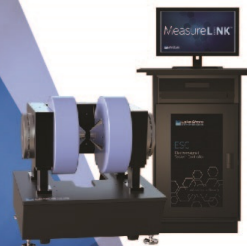
Highly sensitive and broadband photodetectors based on $WSe_2/MoS_2$ heterostructures with van der Waals contact electrodes
Applied Physics Letters **121**, 023504 (2022); https://doi.org/10.1063/5.0100191

# Graphene/SOI-based self-powered Schottky barrier photodiode array (EP)

A. Yanilmaz,[1,2,3] (iD) M. Fidan,[1,4] (iD) O. Unverdi,[5] (iD) and C. Çelebi[1,a]) (iD)

**AFFILIATIONS**

[1]Quantum Device Laboratory, Department of Physics, Izmir Institute of Technology, Izmir 35430, Turkey
[2]Department of Photonics, Izmir Institute of Technology, Izmir 35430, Turkey
[3]Ermaksan Optoelectronic R&D Center, Bursa 16140, Turkey
[4]Department of Opticianry, İzmir Kavram Vocational School, İzmir 35230, Turkey
[5]Faculty of Engineering, Department of Electrical and Electronic Engineering, Yasar University, Izmir 35100, Turkey

**Note:** This paper is part of the APL Special Collection on Photodetectors Based on Van der Waals Heterostructures and Hybrid 2D Materials.
[a])Author to whom correspondence should be addressed: cemcelebi@iyte.edu.tr

## ABSTRACT

We have fabricated a four-element graphene/silicon on insulator (SOI) based Schottky barrier photodiode array (PDA) and investigated its optoelectronic device performance. In our device design, monolayer graphene is utilized as a common electrode on a lithographically defined linear array of n-type Si channels on a SOI substrate. As revealed by wavelength resolved photocurrent spectroscopy measurements, each element in the PDA structure exhibited a maximum spectral responsivity of around 0.1 A/W under a self-powered operational mode. Time-dependent photocurrent spectroscopy measurements showed excellent photocurrent reversibility of the device with ∼1.36 and ∼1.27 μs rise time and fall time, respectively. Each element in the array displayed an average specific detectivity of around $1.3 \times 10^{12}$ Jones and a substantially small noise equivalent power of ∼0.14 pW/Hz$^{-1/2}$. The study presented here is expected to offer exciting opportunities in terms of high value-added graphene/Si based PDA device applications such as multi-wavelength light measurement, level metering, high-speed photometry, and position/motion detection.

*Published under an exclusive license by AIP Publishing.* https://doi.org/10.1063/5.0092833

Photodiodes based on a graphene/silicon (G/Si) heterojunction have attracted a great deal of attention in the last decade since they exhibit photo-responsivity similar to p–n or p–i–n type Si photodiodes.[1,2] It has been shown that a rectifying Schottky contact with an energy barrier level of around 0.5–0.8 eV is formed when graphene is laid on the surface of bulk Si substrate.[3,4] The G/Si heterojunction operates as a Schottky barrier diode, which is sensitive to light in the spectral range between 400 and 1100 nm due to the bandgap of Si. When graphene is employed as an electrode on Si, it does not only act as an optically transparent conductive layer, but it functions also as a photon absorbing active material similar to metal silicide electrodes used in conventional metal/Si Schottky barrier photodiodes.[5,6] Under light illumination, although a large amount of photons is converted into photo-generated charge carriers in Si, the optical absorbance in graphene (∼2.3%) contributes to light detection as well through internal photoemission over the Schottky barrier. The photo-generated electrons with high enough energies to overcome the Schottky barrier

are accelerated toward the bulk of Si due to the built-in electric field at the interface of G/Si. As the electrons pass through the depletion region of Si, they undergo energy loss processes that prevent them from passing back into the graphene over layer. This results in an effective charge separation and, hence, in a measurable photocurrent and/or photovoltage even under zero-bias (self-powered) conditions. Therefore, the G/Si Schottky photodiode in a self-powered (photovoltaic) mode can operate unconventionally without consuming external power and is a good candidate for solar cells and photo-detection due to the promising application in energy-efficient systems.[7]

A variety of different design strategies have been employed to fabricate single element G/Si based Schottky barrier photodiodes. These include the transfer of monolayer graphene either on oxide-free or on the nanotip patterned surface of bulk Si substrates.[8,9] There are several other approaches relying on the fabrication of these types of photodiodes using silicon-on-insulator (SOI) technology. A SOI structure, which is composed of buried SiO$_2$ (BOX) sandwiched between a

thin Si layer and a thick Si substrate, provides great opportunities for producing G/Si based photodetectors with improved device performance. For example, a bottom-gated SOI transistor with isolated patterned graphene layers on top of a single channel Si has been utilized as a single pixel photodetector to detect light in the visible to the near-infrared range.[10] In a subsequent work, it has been shown that SOI based single pixel G/Si Schottky photodiodes exhibit a maximum spectral responsivity of around 0.26 AW$^{-1}$ at 635 nm peak wavelength and a response time substantially smaller than a microsecond compared to their counterparts fabricated on bulk Si substrates.[11]

In this Letter, we demonstrate that a multi-channel G/Si Schottky barrier photodiode array (PDA) can be fabricated on SOI substrates using standard microfabrication techniques applied in CMOS technology. In our device design, we used the advantage of the BOX layer in SOI, which acts as a well-defined etch-stop and provides an excellent electrical isolation in between laterally aligned neighboring photoactive G/Si elements in the array. In the fabrication process, single layer graphene is utilized as a common electrode on a linear array of multiple n-type Si channels, which were lithographically exposed on a single SOI substrate. Current–voltage (I–V) and wavelength resolved photocurrent spectroscopy measurements showed that each G/Si element in the PDA operates in the self-powered mode and responds to incident light independent of each other. The optoelectronic device parameters, including

spectral responsivity, specific detectivity, noise equivalent power, and response speed of the G/Si PDA sample, were systematically investigated and reported in the Letter.

Figure 1(a) shows a schematic illustration of the SOI based four-element G/Si Schottky PDA fabricated within the scope of this work. The details of graphene growth, characteristic dimensions of Si elements on SOI, and device fabrication steps can be found in the supplementary material. For the experiments $10 \times 10 \ mm^2$ sized, $10 \ \mu m$ thick n-doped photo-active silicon [Si (100)] SOI substrates (specification $\rho = 1$–$5 \ \Omega \ cm$, nominal doping level $N_d \approx 2 \times 10^{15} \ cm^{-3}$) were used. The device structures were prepared by using a photolithography technique. A dry etching method (Reactive Ion Etching (RIE), Sentech, Inc.) was used to reach the oxide layer (BOX) and to obtain an array of n-Si channels on SOI substrates. Following the fabrication of a Si array, the windows for metal contact pads were defined by an additional lithography step. After Cr (5 nm)/Au (80 nm) metals were evaporated both on the n-Si side and on the $SiO_2$ side of the SOI substrates with a thermal evaporation system, a liftoff process was applied to get the linear array device structure depicted in Fig. 1(a). Chemical vapor deposition (CVD) grown monolayer graphene with a surface coverage of higher than 95% was transferred on the arrayed SOI substrate by using the same graphene transfer method in Ref. 12 The graphene layer in the device design was employed as a hole collecting common electrode and acted as the active region when interfaced with
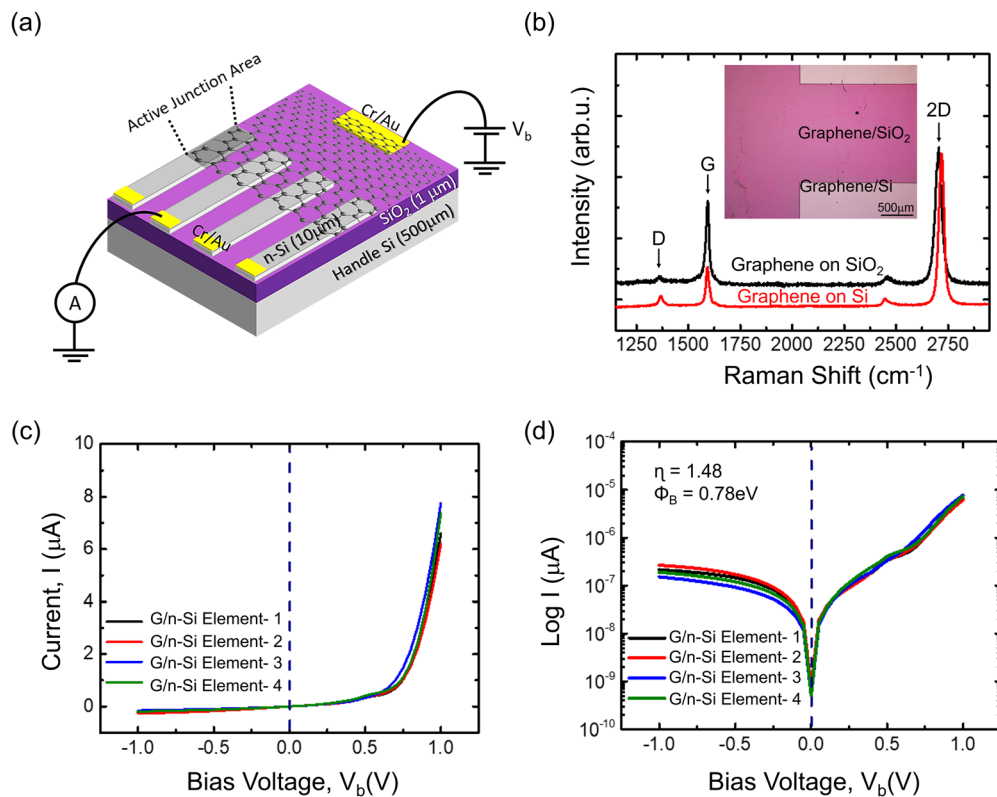


**FIG. 1.** (a) The schematic of the fabricated G/n-Si PDA device. (b) Raman spectrum of transferred graphene on Si and $SiO_2$ sides of the SOI substrate. (The inset shows the optical micrograph of the region selected for acquiring a Raman spectrum of the graphene layer.) (c) The I–V curve of the device in the dark and (d) the ln(I)–V plot, which was used to extract the ideality factor and Schottky barrier height of each element.

the arrayed n-Si elements on the SOI substrate. It should be noted that although the dimension of the graphene layer (employed as the common electrode) is limited by the small volume of our graphene growth setup, the technique presented here is compatible for the fabrication of industrial scale G/Si PDA structures, which require large scale graphene production and transfer processes.[13] For future studies, it might be also interesting to produce G/Si PDA devices with disconnected individual graphene electrodes on every single Si element in the array. In this case, disconnected and separated graphene electrodes can be laterally patterned on arrayed Si channels with the technique developed in Ref. 14.

After the transfer process, the presence of graphene on Si and SiO$_2$ regions of the SOI substrate was determined by single point Raman spectroscopy measurements taken under a laser with 532 nm excitation wavelength. As shown in Fig. 1(b), graphene related D, G, and single Lorentzian shaped 2D peaks were identified in all the obtained Raman spectra. Strong G peak and weak D peak indicate good graphitic quality, and the ratio of 2D peak intensity with G peak intensity ($I_{2D}/I_G > 2$) confirms that graphene is monolayer[15] on the arrayed SOI substrate. Following the Raman analysis, I–V measurements of each G/n-Si element on the SOI substrate were conducted one by one under dark conditions, and the obtained results are plotted in Fig. 1(c). All the I–V curves exhibit strong rectifying characteristics of a typical Schottky barrier diode but with slightly different current levels varying in the forward bias region [Fig. 1(c)]. For a detailed comparison, the I–V data were plotted in the semi-logarithmic scale as shown in Fig. 1(d). From the ln(I)–V plots, the dark current ($I_d$) of the G/n-Si elements was extracted as ~0.5 nA in average. In the forward-bias range, although the current increases linearly at very small voltages in accordance with the well-known thermionic-emission model, the deviation from linearity observed at relatively high voltages (e.g., $V_b > 0.1$ V) is due to the series resistance contributions from the underlying n-Si element. The slight difference seen at the reverse bias saturation currents suggests only a small variation in the rectification strength of the G/n-Si heterojunction. Using the method developed by Cheung et al.,[16] the average Schottky barrier height ($\Phi_B$) and the ideality factor ($\eta$) of the PD elements were extracted from the linear forward-bias region of the ln(I)–V plot as 0.78 eV and 1.48, respectively. These two diode parameters are consistent with those of G/Si based Schottky barrier photodiodes fabricated on thick and bulk n-Si substrates.[17,18]

The photoresponse of each individual G/n-Si element in the PDA was characterized separately under illumination of light with 660 nm wavelength. For the experiments, an LED source was coupled to a fiber optic cable with 600 μm core diameter to maintain local illumination on each G/n-Si element and on SiO$_2$ regions between them as depicted in Fig. 2(a). To avoid possible optical crosstalk between neighboring n-Si elements, the distance between the sample and the tip of the fiber optic cable was kept at ~1 mm to ensure well-defined spot size and to minimize possible back reflections that may, respectively, arise from the illuminated Si surface and the metallic tip of the fiber optic probe used in the experiments. As seen in the ln(I)–V plots [Fig. 2(c)], all the G/n-Si elements displayed a clear photoresponse with measurable photocurrent ($I_{pc}$) under light illumination even at zero-bias ($V_b = 0$ V). The shift of the minimum current seen at the forward bias range corresponds to the open circuit voltage ($V_{oc}$) and is typical for self-powered G/n-Si photodiodes operating in the

self-powered mode.[19] It is known that, when the G/n-Si heterojunction is subject to light illumination, the incident photons pass through the optically transparent graphene electrode are absorbed by the Si substrate underneath. As a result of photo excitation, electron–hole pairs are created at the depletion region. In the case of zero bias voltage, the depletion region width ($X_d$) is calculated as ~1 μm for a built-in potential ($V_{bi}$) of 0.7 V and a nominal donor doping concentration ($N_d$) of ~$2 \times 10^{15}$ cm$^{-3}$. The photo-generated charge carriers are separated due to an effective built-in electric field at the interface between the graphene layer and n-Si. Optically excited charge carriers in graphene gain sufficient energy to overcome the Schottky barrier formed at the G/n-Si interface and lead to a photocurrent[20] even at zero-bias [Fig. 2(b)]. From the I–V plot shown in Fig. 2(c), zero-bias $I_{pc}$ of G/n-Si elements was determined to be varying in a range between 1.6 and 3.1 μA. In the case when the light source is brought on the SiO$_2$ regions located in between two neighboring active elements [Fig. 2(a)], the zero-bias currents of G/n-Si elements were measured as ~ 3.1–9.4 × $10^{-9}$ A. Compared to the corresponding $I_d$ values, such a slight increase in the measured currents is due to a trace amount of light, which was randomly reflected back from the tip of the metallic casing
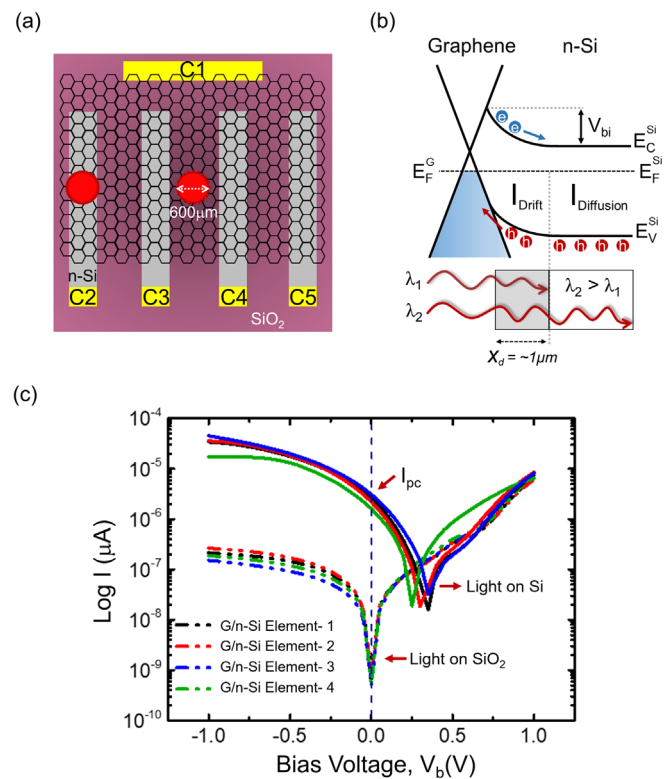


**FIG. 2.** Optical crosstalk measurement results of G/n-Si Schottky PDAs: (a) local illumination on each G/n-Si element and illumination on SiO$_2$ regions located in between two neighboring active elements; (b) the schematic illustration of the energy band diagram for the self-powered G/n-Si Schottky PDAs under light illumination and cross section through the top silicon layer, indicating light and optical carrier contributions of drift and diffusion current, $I_{drift}$ and $I_{diffusion}$, respectively; and (c) ln(I)–V measurements acquired on G/n-Si elements and on SiO$_2$ regions between them. (C1: common graphene contact and C2, C3, C4, and C5 represent the contacts on n-Si).

of the fiber optic probe onto the surface of photoactive G/n-Si elements. When the effects of reflected light on the measured current are ignored, it is possible to state that there is almost no crosstalk between neighboring G/n-Si elements in the array.

The spectral responsivity (R) is one of the most important parameters for the light sensing capability of a photodiode and can be written as[21]

$$R = \frac{I_{pc} - I_d}{P(\lambda)}, \quad (1)$$

where P is the optical power of incident light at certain wavelength ($\lambda$). The spectral responsivity of each element in the PDA was measured at $V_b = 0\,V$ as a function of $\lambda$ of the incident light varied in the spectral range between 400 and 1050 nm. The obtained results were compared with those of a typical G/n-Si based reference PD fabricated on a 500 $\mu$m thick bulk n-Si having the same doping concentration as the n-Si layer on the SOI substrate. As seen in Fig. 3(a), the maximum spectral responsivity ($R_{max}$) of the reference PD and G/n-Si element with a 10 $\mu$m thick active Si layer were determined as $\sim$0.7 AW$^{-1}$ ($\lambda_{Rmax} = 905\,nm$) and $\sim$0.1 AW$^{-1}$ ($\lambda_{Rmax} = 660\,nm$), respectively. The difference in the maximum spectral responsivities is due to the active junction area of the reference PD ($\sim$20 mm$^2$), which is larger than that of each G/n-Si element ($\sim$3 mm$^2$) in the array. It has been shown that the larger active junction area leads to a wider depletion

region, which promotes the effective separation/collection of the photo-generated charge carriers at the depletion region. As a consequence of enhanced charge separation efficiency, $I_{pc}$ and R increase proportionally with the size of the active junction area.[22] The blue shift observed in the maximum spectral response wavelength for G/n-Si elements in the array is due to a thin Si layer. Compared to bulk Si, the absorption of light is limited to shorter wavelengths in the case of thin Si layer as discussed in Ref. 23.

For a detailed comparison, normalized spectral responsivities of the reference PD and a typical G/n-Si element were plotted in Fig. 3(b). Different from that of the reference PD, the spectral responsivity of the G/n-Si element exhibits two maxima located at around 660 and 780 nm wavelengths and decays earlier for the wavelengths above 780 nm. The observed difference in the two distinct spectral responsivity characteristics can be understood in terms of the penetration depth of light and reduced absorption coefficient of the Si layer on SOI. The photoresponse contribution is only provided by the absorption of incident light in the active thin Si layer on SOI when compared with bulk Si. The BOX layer and Si handle make ineffectively the remaining light power for photoresponse gain in the SOI structure.[11] Accordingly, light-trapping concepts that prolong the light path in thick and bulk Si substrates should be considered. Although only the drift currents contribute in shorter wavelengths, diffusion currents become dominant in a longer wavelength regime where the light penetrates deeper into the substrate [Fig. 2(b)]. For G/Si Schottky photodiodes on bulk Si, in which the depletion region is wider compared to that of the G/n-Si element out of thin Si, the spectral responsivity is shifted toward longer wavelengths due to increased amount of the diffusion currents.[8] Because of the fact that the spectral responsivity of G/n-Si elements in the array appears to decline earlier than that of G/Si PD fabricated out of thick and bulk n-Si substrates.[24] As also reported for SOI based single pixel G/Si Schottky PD,[11] the photo-active thin Si forms an optical microcavity on the layered structure of the SOI substrate and causes an oscillating spectral responsivity as displayed in Fig. 3(b). Such an oscillatory behavior arises from constructive and destructive interference effects due to multiple reflections occurred between different interfaces in the SOI structure.[11]

Taking into account the maximum spectral responsivity ($R_{max}$) read at 660 nm wavelength, we also calculated the specific detectivity ($D^*$) and noise equivalent power (NEP) parameters of each active element in the array. Here, $D^*$ is defined as the weakest level of light detected by a photodiode with a junction area (A) of 1 cm$^2$ and is determined by[24,25]

$$D^* = \frac{A^{1/2}R}{\sqrt{2eI_d}}, \quad (2)$$

and NEP is the incident power required to obtain a signal-to-noise ratio of 1 at a bandwidth of 1 Hz and is calculated by[22,26]

$$NEP = \frac{A^{1/2}}{D^*}. \quad (3)$$

Considering $R_{max} = 0.1\,AW^{-1}$ and $A = 3\,mm^2$, the average $D^*$ and NEP of the G/n-Si elements were calculated as $\sim$1.3 $\times$ 10$^{12}$ Jones and $\sim$0.14 pW/Hz$^{-1/2}$, respectively. These two photodiode parameters are in good agreement with those of both single pixel G/Si PD on SOI and G/Si PD on bulk Si substrates.[11,22]
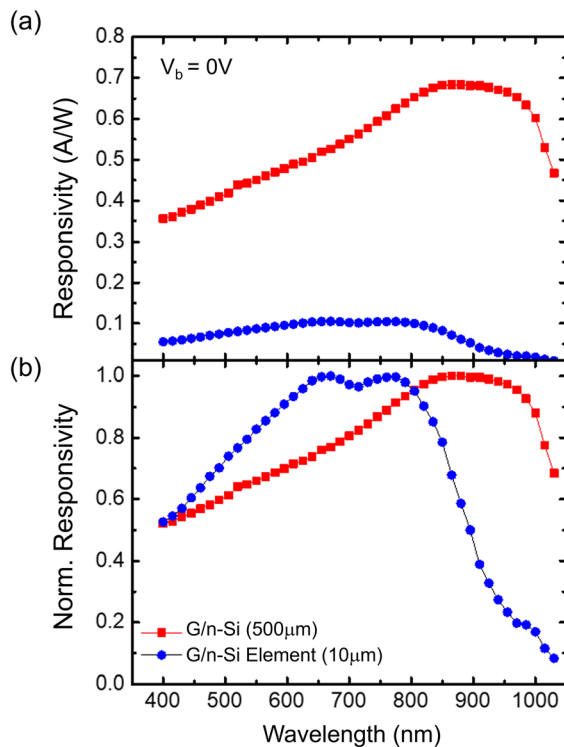


**FIG. 3.** (a) Comparison of the spectral responsivities of a typical G/n-Si element in the PDA device on the SOI substrate (blue) and a reference G/Si Schottky PD fabricated on a 500 $\mu$m thick bulk Si substrate (red) under zero-bias voltage. (b) Comparison of the normalized spectral responsivities of these two devices.
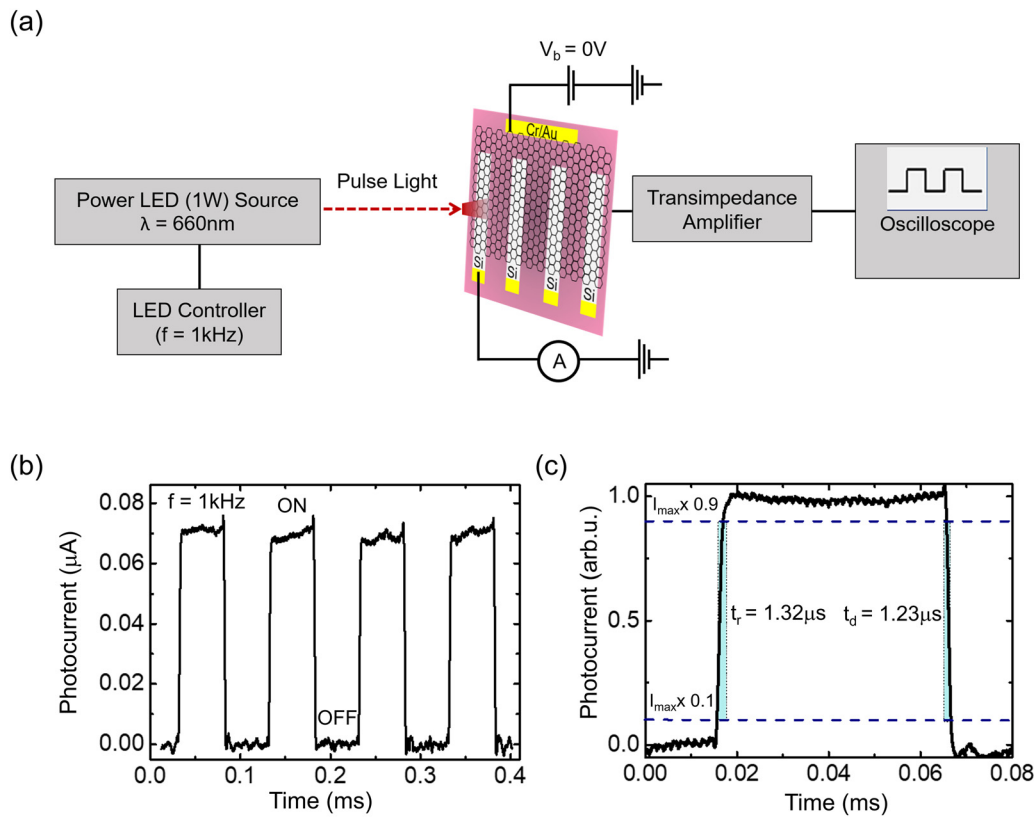
**FIG. 4.** (a) Schematic diagram of the time-resolved photocurrent spectroscopy measurement setup. (b) Time-resolved photocurrent spectrum of an individual G/n-Si element under 660 nm wavelength light with 1 kHz switching frequency at zero-bias voltage. (c) One cycle time-resolved photocurrent spectrum of an individual G/n-Si element in the PDA device.

For determining the response speed and 3-dB bandwidth ($B_w$) of the active elements in the PDA, we conducted time-resolved photocurrent spectroscopy measurements using the experimental setup illustrated in Fig. 4(a). The measurements revealed that all the elements have excellent photocurrent on/off reversibility as seen in Fig. 4(b). Rise time ($t_r$) and decay time ($t_d$) of each individual element in the array were determined from single pulse response measurements taken under 660 nm wavelength light pulsed with 1 kHz frequency. Here, $t_r$ is defined as the range that the photocurrent rises from 10% to 90% of its maximum and $t_d$ is defined similarly. A typical example for single pulse response measurement on an individual G/n-Si element is shown in Fig. 4(c). Considering the measurements taken on other individual G/n-Si elements in the PDA, the average $t_r$ and $t_d$ were determined as ~1.36 and ~1.27 $\mu$s, respectively. Using the relation $B_w = 0.35/t_r$, the average 3-dB $B_w$ of the G/n-Si elements in the array was

calculated as ~257 kHz. For convenience, all the obtained performance characteristics of each element in the PDA device structure are listed in Table I. The comparison of key parameters such as the preferable R, D*, and NEP, low noise, rapid response time of G/n-Si PDA obtained (under zero bias voltage) in this work with previous reported G/Si PDs can be found in Table S1 of the supplementary material.

In conclusion, we have demonstrated the G/n-Si based multi-channel Schottky barrier linear PDA on a conventional SOI substrate and investigated its optoelectronic characteristics. In the PDA device structure, monolayer graphene is utilized as the common electrode on the four-element n-Si array fabricated with a two-step photolithography process on a single SOI structure. The I–V measurements taken under dark ambient revealed a rectifying Schottky contact between the graphene electrode and each n-Si element in the array. Each of the individual element in the array exhibited a clear photo-response even

**TABLE I.** Summary of the performance parameters for four-element G/n-Si Schottky PDAs under 660 nm wavelength light at 0 V bias voltage (junction area, 3 mm$^2$).

| Element ID | $I_{dark}$ (nA) | Rmax (A/W) | D* ($10^{12}$) (Jones) | NEP (pW/Hz$^{-1/2}$) | $t_r$ ($\mu$s) | $t_d$ ($\mu$s) | 3-dB $B_w$ (kHz) |
|---|---|---|---|---|---|---|---|
| G/n-Si element-1 | 0.6 | 0.11 | 1.38 | 0.125 | 1.40 | 1.28 | 250 |
| G/n-Si element-2 | 0.8 | 0.10 | 1.29 | 0.161 | 1.38 | 1.31 | 253 |
| G/n-Si element-3 | 0.5 | 0.10 | 1.26 | 0.127 | 1.32 | 1.23 | 265 |
| G/n-Si element-4 | 0.3 | 0.09 | 1.25 | 0.138 | 1.33 | 1.21 | 263 |

under (zero-bias) self-powered operational mode similar to that observed for the graphene/SOI based single pixel Schottky barrier photodiode, which was previously reported in the literature. We showed that multiple G/n-Si photodiodes, operating independently from each other on a single SOI substrate, can be produced simply by employing single layer graphene as the common electrode. This study offers exciting opportunities for the realization of high-value added technological applications based on motion and position detection, imaging, and spectrophotometry in which graphene and SOI technology can be used together.

See the supplementary material for further experimental details, device fabrication process, along with corresponding figures and comparison of G/n-Si Schottky barrier PDA with previously reported single element G/n-Si photodiodes fabricated on bulk Si and on SOI substrates.

## AUTHOR DECLARATIONS

### Conflict of Interest

The authors have no conflicts to disclose.

### Author Contributions

**Alper Yanilmaz:** Data curation (equal); Formal analysis (equal); Investigation (equal); Writing – original draft (equal). **Mehmet Fidan:** Formal analysis (equal); Investigation (equal). **Özhan Ünverdi:** Funding acquisition (equal); Supervision (equal); Validation (equal); Writing – review and editing (equal). **Cem Çelebi:** Investigation (equal); Supervision (equal); Validation (equal); Writing – review and editing (equal).

## DATA AVAILABILITY

The data that support the findings of this study are available from the corresponding authors upon reasonable request.

## REFERENCES

[1] Y. Dong, W. Wang, D. Lei, X. Gong, Q. Zhou, S. Y. Lee, W. K. Loke, S. F. Yoon, E. S. Tok, and G. Liang, Opt. Express **23**, 18611 (2015).

[2] A. V. Shevlyagin, D. L. Goroshko, E. A. Chusovitin, K. N. Galkin, N. G. Galkin, and A. K. Gutakovskii, Sci. Rep. **5**, 14795 (2015).

[3] D. Sinha and J. U. Lee, Nano Lett. **14**, 4660 (2014).

[4] H.-Y. Kim, K. Lee, N. McEvoy, C. Yim, and G. S. Duesberg, Nano Lett. **13**, 2182 (2013).

[5] S. Tongay, M. Lemaitre, X. Miao, B. Gila, B. R. Appleton, and A. F. Hebard, Phys. Rev. X **2**, 011002 (2012).

[6] R. Yan, Q. Zhang, O. A. Kirillov, W. Li, J. Basham, A. Boosalis, X. Liang, D. Jena, C. A. Richter, and A. C. Seabaugh, Appl. Phys. Lett. **102**, 123106 (2013).

[7] Y. Miyoshi, Y. Fukazawa, Y. Amasaka, R. Reckmann, T. Yokoi, K. Ishida, K. Kawahara, H. Ago, and H. Maki, Nat. Commun. **9**, 1279 (2018).

[8] H. Selvi, N. Unsuree, E. Whittaker, M. P. Halsall, E. W. Hill, A. Thomas, P. Parkinson, and T. J. Echtermeyer, Nanoscale **10**, 3399 (2018).

[9] A. D. Bartolomeo, F. Giubileo, G. Luongo, L. Iemmo, N. Martucciello, G. Niu, M. Fraschke, O. Skibitzki, T. Schroeder, and G. Lupina, 2D Mater. **4**, 015024 (2016).

[10] C.-H. Liu, Y.-C. Chang, F. Cai, M.-B. Lien, D. Zhang, W. Lu, T. B. Norris, and Z. Zhong, in Proeedings of the Conferenceon Lasers Electro-Optics, 2016.

[11] H. Selvi, E. W. Hill, P. Parkinson, and T. J. Echtermeyer, Nanoscale **10**, 18926 (2018).

[12] N. Şahan, M. Fidan, and C. Çelebi, Appl. Phys. A **126**, 1–6 (2020).

[13] N. Avishan, N. Hussain, and F. Nosheen, Mater. Innovations **2**(1), 15–25 (2022).

[14] Y. Xu, A. Ali, K. Shehzad, N. Meng, M. Xu, Y. Zhang, X. Wang, C. Jin, H. Wang, Y. Guo, Z. Yang, B. Yu, Y. Liu, Q. He, X. Duan, X. Wang, P. Tan, W. Hu, H. Lu, and T. Hasan, Adv. Mater. Technol. **2**, 1600241 (2017).

[15] J. S. Park, A. Reina, R. Saito, J. Kong, G. Dresselhaus, and M. S. Dresselhaus, Carbon **47**, 1303 (2009).

[16] S. K. Cheung and N. W. Cheung, Appl. Phys. Lett. **49**, 85 (1986).

[17] S. Riazimehr, A. Bablich, D. Schneider, S. Kataria, V. Passi, C. Yim, G. S. Duesberg, and M. C. Lemme, Solid State Electron. Lett. **115**, 207 (2016).

[18] Y. Wang, S. Yang, A. Ballesio, M. Parmeggiani, A. Verna, M. Cocuzza, C. F. Pirri, and S. L. Marasso, J. Appl. Phys. **128**, 014501 (2020).

[19] A. D. Bartolomeo, Phys. Rep. **606**, 1–58 (2016).

[20] E. V. Castro, H. Ochoa, M. I. Katsnelson, R. V. Gorbachev, D. C. Elias, K. S. Novoselov, A. K. Geim, and F. Guinea, Phys. Rev. Lett. **105**, 266601 (2010).

[21] J. Li, L. Niu, Z. Zheng, and F. Yan, Adv. Mater. **26**, 5239 (2014).

[22] M. Fidan, Ö. Ünverdi, and C. Çelebi, Sens. Actuators, A **331**, 112829 (2021).

[23] A. Ali, K. Shehzad, H. Guo, Z. Wang, P. Wang, A. Qadir, W. Hu, T. Ren, B. Yu, and Y. Xu, in IEEE International Electron Devices Meeting (IEDM) (IEEE, 2017), pp. 8.6.1–8.6.4.

[24] H. Aydın, S. B. Kalkan, C. Varlikli, and C. Çelebi, Nanotechnology **29**, 145502 (2018).

[25] X. Wan, Y. Xu, H. Guo, K. Shehzad, A. Ali, Y. Liu, J. Yang, D. Dai, C.-T. Lin, and L. Liu, npj 2D Mater. Appl. **1**, 4 (2017).

[26] X. Li, M. Zhu, M. Du, Z. Lv, L. Zhang, Y. Li, Y. Yang, T. Yang, X. Li, and K. Wang, Small **12**, 595 (2016).